HHS Public Access

Author manuscript

Fungal Genet Biol. Author manuscript; available in PMC 2017 May 19.

Published in final edited form as:

Fungal Genet Biol. 2017 March ; 100: 22–32. doi:10.1016/j.fgb.2017.01.005.

Paracoccidioides spp. catalases and their role in antioxidant defense against host defense responses

Diana Tamayo[1,2,3], **José F. Muñoz**[1,2,4], **Agostinho J. Almeida**[1,5], **Juan D. Puerta**[1], **Ángela Restrepo**[1], **Christina A. Cuomo**[4], **Juan G. McEwen**[1,6], and **Orville Hernández**[1,3,7]

[1]Cellular and Molecular Biology Unit, Corporación para Investigaciones Biológicas, Medellín, Colombia

[2]Institute of Biology, Universidad de Antioquia, Medellín, Colombia

[3]School of Microbiology, Universidad de Antioquia, Medellín, Colombia

[4]Broad Institute of MIT and Harvard, Cambridge, Massachusetts, USA

[5]Department of Biological Sciences, School of Sciences, Universidad EAFIT, Medellín, Colombia

[6]School of Medicine, Universidad de Antioquia, Medellín, Colombia

[7]MICROBA research group. School of Microbiology, Universidad de Antioquia, Medellín, Colombia

Abstract

Dimorphic human pathogenic fungi interact with host effector cells resisting their microbicidal mechanisms. Yeast cells are able of surviving within the tough environment of the phagolysosome by expressing an antioxidant defense system that provides protection against host-derived reactive oxygen species (ROS). This includes the production of catalases (CATs). Here we identified and analyzed the role of CAT isoforms in *Paracoccidioides*, the etiological agent of paracoccidioidomycosis. Firstly, we found that one of these isoforms was absent in the closely related dimorphic pathogen *Coccidioides* and dermatophytes, but all of them were conserved in *Paracoccidioides, Histoplasma* and *Blastomyces* species. We probed the contribution of CATs in *Paracoccidioides* by determining the gene expression levels of each isoform through quantitative RT-qPCR, in both the yeast and mycelia phases, and during the morphological switch (transition and germination), as well as in response to oxidative agents and during interaction with neutrophils. *PbCATP* was preferentially expressed in the pathogenic yeast phase, and was associated to the response against exogenous H_2O_2. Therefore, we created and analyzed the virulence defects of a knockdown strain for this isoform, and found that *CATP* protects yeast cells from H_2O_2 generated *in vitro* and is relevant during lung infection. On the other hand, *CATA* and *CATB* seem to contribute to ROS homeostasis in *Paracoccidioides* cells, during endogenous oxidative stress. CAT isoforms in *Paracoccidioides* might be coordinately regulated during development and dimorphism, and differentially expressed in response to different stresses to control ROS homeostasis during the infectious process, contributing to the virulence of *Paracoccidioides*.

Corresponding author: Orville Hernández, Ph.D. orville.hernandez@udea.edu.co.

Keywords

Paracoccidioides spp.; dimorphic fungal pathogens; antisense RNA; catalases; peroxide; endogenous and exogenous ROS

1. Introduction

Dimorphic fungal pathogens are the commonest cause of invasive fungal diseases worldwide infecting immunocompetent and immunocompromised hosts and accounting for several million infections each year (Buitrago and Cuenca-Estrella, 2012; Colombo et al., 2011; Sifuentes-Osornio et al., 2012). The largest cluster of thermally dimorphic fungi includes the genera *Histoplasma*, *Blastomyces*, *Coccidioides*, and *Paracoccidioides* in the order Onygenales. Dimorphism in these species involves the ability to switch between two different morphologies in response to external stimuli, primarily temperature. At 22–25°C, they grow as molds that produce infectious conidia, while at 37°C they grow as yeast-like forms (*Histoplasma, Blastomyces* and *Paracoccidioides*) or as spherules (*Coccidioides*) (Boyce and Andrianopoulos, 2015).

The ability of these pathogens to cause disease entails their capability to survive inside their human host (Missall et al., 2004). They have evolved mechanisms that allow them to adapt and grow within the host and cause disease (de Oliveira et al., 2015; Perez-Nadales et al., 2014). Once inside the host, dimorphic fungi are challenged by a higher temperature that not only induces the transition to the parasitic form, but also increases the generation of Reactive Oxygen Species (ROS), as well as the oxidative damage resulting from the inhibition of the mitochondrial respiration (Martins et al., 2011; Ruiz et al., 2011; Vacca et al., 2004). In addition, the fungus faces other sources of oxidative stress from phagocytic cells, mainly from neutrophils (PMNs) and activated macrophages (Robinson et al., 2004).

These pathogenic fungi are able of surviving within the tough conditions imposed by phagocytic cells, especially when the formation of the phagolysosome takes place. This suggests the presence of an antioxidant defense system that provides protection to the fungus against host-derived ROS (Giles et al., 2006). Oxidative stress has been proven to trigger changes in gene expression, changes that are required for expression of fungal virulence and pathogenicity traits, and include the expression of superoxide dismutases (SODs) (Tamayo et al., 2016; Youseff et al., 2012), glutathione/thioredoxin system, cytochrome C peroxidase (CCP) (Parente-Rocha et al., 2015) and catalases (CATs) (Chagas et al., 2008; Holbrook et al., 2013). CATs are ubiquitous in aerobic organisms and provide protection against the oxidative stress resulting from exogenous and endogenous ROS (Chelikani et al., 2004; Giles et al., 2006). In fungal pathogens such as *Blastomyces, Histoplasma, Paracoccidioides*, among others, CAT genes encode a small family of proteins including *CATA*, *CATB* and *CATP*, which catalyze the decomposition of hydrogen peroxide (H_2O_2) into oxygen and water (Chagas et al., 2008; Holbrook et al., 2013; Loew, 1900; Munoz et al., 2015). H_2O_2 toxicity relies on the products formed during its interaction with ferrous iron (Fe^{2+}) via the Fenton reaction. In the presence of Fe^{2+}, H_2O_2 is reduced to hydroxyl anion (OH^-) and hydroxyl radical (·OH). Although the latter radical has a fleeting nature and a short diffusion

distance, it is highly nonselective and is the most active oxidant among the ROS. Due to its transience, living organisms have not developed specific enzymatic systems for its detoxification; thus, the best way to protect the cell against the deleterious effects of this radical is preventing its production (Imlay et al., 1988; Lushchak, 2011). In this way, the presence of CATs allow cells to destroy H_2O_2 radicals, reducing the probability of converting the peroxide produced by phagocytic cells into more potent and potentially toxic microbicidal reactive oxygen intermediates. Consequently, in the absence of these H_2O_2-detoxifying enzymes, increased fungal damage can be expected to occur (Henriet et al., 2011).

Paracoccidioides is the etiological agent of paracoccidioidomycosis (PCM), one of the most prevalent systemic mycosis in Latin America (Colombo et al., 2011). In endemic areas, the estimated incidence is approximately one to three cases per 100.000 inhabitants per year (Martinez, 2015). Phylogenetic analyses led to discover that the *Paracoccidioides* genus compromises two species: *P. brasiliensis* and *P. lutzii* (Teixeira et al., 2009). In turn, *P. brasiliensis* has been classified into different phylogenetic lineages (S1, PS2, PS3 and PS4) (Hahn et al., 2014; Matute et al., 2006; Teixeira et al., 2014), and recently using population genomics, we identified a deep split in the S1 group, breaking it into two lineages named S1a and S1b (Munoz et al., 2016). Isolates among the *P. brasiliensis* and *P. lutzii* phylogenetic lineages can infect humans, but they vary in their virulence and induce different host immune responses (Gegembauer et al., 2014; Scorzoni et al., 2015).

Recently, we demonstrated that *Paracoccidioides* cells produce six SODs isoforms. From these, *PbSOD1* and *PbSOD3* were involved in the fungus response against oxidative stress, and were required for virulence in a mouse model of infection (Tamayo et al., 2016). In addition to the latter genes, *Paracoccidioides* genome also encodes three CAT genes. Moreira *et al.* 2004, Chagas *et al.* 2008 and 2010 studied the CATs in this dimorphic fungus. These works suggested the possible role of *CATP* in defense against the oxidative stress produced during the host-pathogen interactions (Chagas et al., 2010; Chagas et al., 2008; Moreira et al., 2004). However, until now, the precise role of this enzyme had remained elusive due to lack of feasible genetic molecular tools that could be applied to the study of the *Paracoccidioides* genus, allowing specifically target candidate genes. Thus, in the present study, we aimed to better understand the role of these enzymes during adaptation to the host's environment, specifically *CATP*.

We initially identified and analyzed the sequences of the CAT gene family members in *Paracoccidioides* and other dimorphic fungal pathogens from Onygenales. Subsequently, we studied the gene expression of the three isoforms and the susceptibility of *Paracoccidioides* yeast cells to H_2O_2. *P. brasiliensis* strain ATCC 60855 was used to analyze the role of these catalases under different conditions, including the morphological switch, exposure to oxidative stress-inducing agents, and during interaction with human PMNs. Subsequently, the antisense RNA counterpart for *CATP* (*PbCATP*-aRNA) was used to facilitate the functional tests performed here. The data here presented shows that *PbCATP* seems to play an important role in the removal of H_2O_2 generated via different stimuli. In line with previous studies performed in our laboratory, these results suggest that CATs and other scavenger enzymes such as SODs (Tamayo et al., 2016) are differentially expressed during

cell growth and dimorphism, as well as in response to distinct external stresses and within the host.

2. Experimental procedures

2.1. Identification and sequence analysis of CAT isoforms

In order to identify and classify the CAT isoforms present in the genomes of *Paracoccidioides* and other dimorphic pathogenic fungi, we used bidirectional BLAST analysis v2.2.28+ with default parameters to identify sequence similarities (Altschul et al., 1997), and ortholog matrices generated with OrthoMCL v1.4 with a markov inflation index of 1.5 and a maximum e-value of 1e-5 using whole genome gene sets (Li et al., 2003).

We studied one representative strain from each of the lineages of *Paracoccidioides*. Pb18, P03 and Pb01 were chosen to represent *P. brasiliensis* (S1, PS2) and *P. lutzii* lineages, respectively (Desjardins et al., 2011; Munoz et al., 2014). For the PS3 lineage, and the recently described PS4, we used the gene set of PbCNH and Pb300 respectively (Munoz et al., 2016). In addition, we identified CAT gene family orthologs in related dimorphic fungi such as *Coccidioides immitis*, *C. posadassi* and *Emmonsia*, from dermatophytes *Trichophyton rubrum* and *Microsporum gypseum*, and three *Aspergillus* species as outgroup (Table S1). For all the identified CAT isoforms, protein domain conservation analyses were done using InterProScan (Zdobnov and Apweiler, 2001), by sequence comparison with InterPro collection of protein signature databases in the EMBL-EBI (http://www.ebi.ac.uk/interpro/). Multiple sequence alignments were constructed using Muscle (Edgar, 2004), and phylogenetic trees were constructed employing a distance computation method (Neighbor-joining) (Saitou and Nei, 1987). Other features in the gene/protein sequences and annotations of the CAT isoforms were identified using SignalP 4.1 (Petersen et al., 2011), TargetP 1.1 (Emanuelsson et al., 2000) and PTS1 Predictor (Neuberger et al., 2003).

2.2. Microorganisms and growth conditions

At least one representative isolate from each phylogenetic lineages of *Paracoccidioides* spp. was used (Table 1). *P. brasiliensis* knockdown strains employed in this study were derived from the background strain ATCC 60855 (PbWT). *Paracoccidioides* yeast cells were maintained by sub-culturing in brain heart infusion (BHI) supplemented with 1% glucose (Beckton Dickinson and Company, Sparks, MD), under constant agitation at 36°C, and at 20°C for the mycelia form, unless otherwise indicated. *P. brasiliensis* conidia were produced and purified using the glass-wool filtration protocol, as described previously by Restrepo *et al.* (Restrepo et al., 1986). In order to induce and evaluate the transition processes (conidia to yeast (C-Y); mycelia to yeast (M-Y)) and the germination process (yeast to mycelia (Y-M)), cells were incubated at 36°C or at 20°C, respectively, during 3, 12, 48 and 96 h, and kept under constant agitation in a flask containing BHI, as previously reported by us (Garcia et al., 2009; Tamayo et al., 2016). It is important to note that during the morphological switch several fungal morphotypes coexist. Cultures during M-Y transition are characterized by the presence of hyphae, differentiating hyphae (chlamydospore-like cells), transforming yeast (production of multiple buds by the chlamydospore) and mature, multibudding yeast (Nunes, Costa de Oliveira et al. 2005). During C-Y transition, cultures are characterized by the

presence of conidia, intermediate cells and yeast cells. After 12 h, intermediate cells are present, from 48 h onwards it is possible to observe the characteristic yeast cells, although, they are more abundant at 72 h. Regarding to the C-M germination, conidia began to germinate approximately at 24 h and the formation of branched mycelia occurs after 96 h (Hernandez et al., 2011a; Hernandez et al., 2011b). Samples were collected for RNA extraction and quantification of gene expression analyses during evaluated time points (Tamayo et al., 2016).

We used *Agrobacterium tumefaciens* strain LBA1100 (Beijersbergen et al., 1992) as the recipient for the binary vectors. Bacterial cells were maintained at 28°C in Luria–Bertani (LB) medium containing kanamycin (100 mg/ml). *Escherichia coli* DH5α was grown at 36°C in LB medium supplemented with kanamycin (50 mg/ml), and used as the host for plasmid amplification and cloning.

2.3. Real-time RT-qPCR analysis

Total RNA was obtained using the Trizol reagent (Invitrogen®) according to manufacturer's instructions. As formerly described (Tamayo et al., 2016), the total RNA obtained was treated with DNase I (Thermo Scientific®) and tested using a conventional PCR with β-tubulin primers to confirm the absence of chromosomal DNA contamination (Goldman et al., 2003; Tamayo et al., 2016). cDNA was synthesized using 2 μg of total RNA with Maxima® First Strand cDNA synthesis kit for RT-qPCR, according to the manufacturer's instructions (Fermentas®) (Tamayo et al., 2016).

Real-time PCR was carried out using a Maxima® SYBR Green/Fluorescein qPCR Master Mix (2X; qRT-PCR) kit with SYBR green, according to the manufacturer's instructions (Fermentas®). The CFX96 real time PCR detection system (Bio-Rad, Hercules, CA) was used to measure gene expression level of CAT isoforms encoded into the *Paracoccidioides*' genome. Primers were designed in order to anneal properly to each CAT transcript (Table S2). Additionally, in Pb60855, CAT isoforms were evaluated in cells undergoing the transition (C-Y and M-Y) as well as in the germination processes (C-M and Y-M). We also evaluated gene expression in knockdown strains for *PbCATP* gene, and in *P. brasiliensis* cells carrying the empty binary vector as a control (PbEV60855, see below construction of knockdown and empty vector strains). Finally, we performed melting curve analysis after the amplification phase. The β-tubulin gene (*TUBE3*, housekeeping gene) was used in order to normalize the expression value of each CAT isoform. We also used the elongation factor 3 (*TEF3*) as a second normalizer control, finding no differences when compared with *TUBE3*, as previously reported by us (Tamayo et al., 2016). Each experiment was done in triplicate, and the expression level was measured three times.

2.4. Construction of *P. brasiliensis PbCATP-a*RNA yeast cells

DNA from PbWT was extracted from yeast cells cultures during exponential growth. We employed a Platinum high-fidelity Taq DNA polymerase (Invitrogen®) to amplify antisense RNA (aRNA) fragments, designed on the sequence of *PbCATP* gene (PADG_00324). Two regions of the gene were selected in order to design six different aRNA fragments and generate the knockdown strains. Five of them were targeted at exon four (80, 120, 92, 106

and 100-bp for *PbCATP*-AS1, AS2, AS3, AS4 and AS5, respectively) and one at exon three (85-bp for *PbCATP*-AS6). *P. brasiliensis* plasmid construction for aRNA and *A. tumefaciens*-mediated transformation (ATMT) were performed as previously described (Almeida et al., 2007). Briefly, the amplified *PbCATP* aRNA oligonucleotide was inserted into the pCR35 plasmid under the control of the Calcium Binding Protein 1 (*CBP*-1) promoter region from *Histoplasma capsulatum* (Rappleye et al., 2004). The pUR5750 plasmid was used as a parental binary vector to harbor this aRNA cassette within the transfer DNA (T-DNA). The constructed binary vectors were introduced into *A. tumefaciens* LBA1100 ultra competent cells by electroporation as described previously (den Dulk-Ras and Hooykaas, 1995), and isolated by kanamycin selection (100 mg/ml).

In *P. brasiliensis* yeast cells, ATMT was done using *A. tumefaciens* cells harboring the desired binary vector in order to obtain the knockdown strains, and were also transformed with the empty parental vector pUR5750 (PbEV) as a control for the experiments. A 1:10 *P. brasiliensis/A. tumefaciens* ratio was employed during the 3 days period of co-culture at 28°C. Selection of *P. brasiliensis* transformants was performed in BHI solid media containing hygromycin B (Hyg; 200mg/ml) over a 15 days incubation period at 36°C. Randomly selected Hyg resistant transformants were tested for mitotic stability and insertion of the T-DNA. The presence of the hygromycin B resistance cassette was confirmed by PCR analysis to detect an HPH 1000-bp amplification product in PbEV and *PbCATP*-aRNA isolates (Figure S1). Also, *PbCATP*-aRNA and PbEV strains were successively sub-cultured on BHI without hygromicin B (three consecutive rounds) and later placed again under the selective pressure of the hygromicin B (Tamayo et al., 2016).

2.5. Viability and vitality in *P. brasiliensis* yeast cells

Growth curves were performed in BHI broth (100 mL). We adjusted the inoculum to an OD of 0.4 for PbWT, PbEV and *PbCATP*-aRNA yeast cells. Then, cultures were incubated at 36°C and samples were collected at specific time points (0, 3, 6, 12, 24, 48, 72 and 96 h) to determine growth curves by spectrophotometric analysis (OD_{600} nm; SmartSpec Plus (Bio-Rad, Hercules, CA).

Vitality, defined as the ability of yeast cells to metabolize glucose upon late activation of a cell membrane proton pump and subsequent acidification of the medium due to H+ release (Kara, 1987), was evaluated following the protocol reported by Hernandez *et al.* (Hernandez et al., 2010). This protocol was detailed in a previous publication by our group (Tamayo et al., 2016). The assays were performed in triplicates.

2.6. Phenotypic analysis of *Paracoccidioides* strains

For the phenotypic analysis, we tested the sensitivity to hydrogen peroxide in the representative strains of the phylogenetic lineages (*P. brasiliensis* S1, PS2, PS3, PS4 and *P. lutzii*) and in PbWT, PbEV and *PbCATP*-aRNA strains. We used H_2O_2-saturated filter disks, with an inoculum of 1×10^5 *Paracoccidioides* yeast cells dispersed on BHI plates. After inoculation, sterile filter disks were loaded with 20 μl of PBS as a control, and with increasing amounts of H_2O_2 (0.5, 1, 2, 4 and 8 M). Plates were incubated at 36°C with 5%

CO_2 and after eight days we measured the clearing area (Holbrook et al., 2013; Tamayo et al., 2016).

We also tested the sensitivity and gene expression profile of the PbWT strain to extracellular induced-oxidative stress, using 0.5 mM riboflavin (R4500, Sigma), 1mM menadione (M5625, Sigma) and 30 mM hydrogen peroxide (02194057, MP Biomedicals). Briefly, 3×10^6 PbWT yeast cells were inoculated in 20 ml of PBS and incubated for 1 hour at 36°C under constant agitation. For the riboflavin assay, cells were exposed to UV-light in order to induce oxidative stress (Ruane et al., 2004). Following this step, samples were collected for RNA extraction and quantification of gene expression during evaluated conditions was done.

We determined the ability of *P. brasiliensis* cellular extracts to destroy H_2O_2 *in vitro*. PbWT, PbEV and *PbCATP*-aRNA cultures were grown in liquid BHI at 37°C. Three biological replicate yeast cultures were used. We adjusted the inoculum to an OD of 0.4. For extracellular catalase activity, we separated the cell mass by centrifugation (12,000 rpm, 5 min at 4°C) and subsequent filtration by passage through a syringe filter of 0.22 μm. The pellet was washed twice with PBS and suspended in PBS. Cytoplasmic protein was released by breaking cells with 0.5-mm-diameter glass beads. Later, a step of low speed centrifugation (3000 g, 5 min at 4°C) was applied in order to obtain the cell wall fraction (Lambou et al., 2010). To slow down enzymatic destruction, all steps were carried out at 4°C. Protein concentrations were determined using the Bradford method with bovine serum albumin protein as the standard. Catalase activity assays for extracellular and intracellular samples were performed by spectrophotometrically measuring their ability to reduce the H_2O_2 concentration over time. For extracellular fractions, we used 200 μl of the culture supernatants with 800 μl of 15 mM H_2O_2 in 50 mM Na-phosphate buffer (pH 7.2). For extracellular cell-associated fraction, 200 μl of the suspension were added to 800 μl of 15 mM H_2O_2 in 50 mM Na-phosphate buffer. Finally, intracellular activity was determined using 12 μg of total protein. Hydrogen peroxide destruction was measured at 240 nm with correction at 595 nm every 30 s for 5 min and compared to that in a control containing buffer (Holbrook et al., 2013; Tamayo et al., 2016).

2.7. Interaction of *P. brasiliensis* yeast cells with human PMNs (*ex vivo* assay)

Polymorphonuclear neutrophils (PMNs) were isolated from human blood samples taken from healthy volunteers. We used whole blood treated with anticoagulant EDTA. Briefly, a layer 5.0 ml of non-coagulated whole blood was placed over 5.0 ml of Polymorphprep™ in a 12 ml centrifuge tube. Samples were centrifuged for 450 × g for 30 min. The polymorphonuclear fraction was then washed with Hanks' Balanced Salt Solution and centrifuged for 400 × g for 10 min. Finally, PMNs were re-suspended in Dulbecco's Modified Eagle Medium (DMEM; Gibco®), enumerated in hemacytometer and cell viability was determined using trypan blue (Mejia et al., 2015). PMNs were seeded into 24-well tissue culture plate and allowed to adhere for 20 min at 36°C with 5% of CO_2. For inhibition of NADPH-oxidase, 10μM diphenylene iodinium (DPI; D2926, Sigma) was added to PMNs 20 min before infection.

For all assays, we used a ratio of 1:5 for *P. brasiliensis* yeasts:host cells. The interaction was kept at 36°C with 5% of CO_2, for 3h. CATs gene expression was performed and viability was measured via colony forming units (Kurita et al., 1993; Ruiz et al., 2011).

2.8. *In vivo* virulence determination

Isogenic 6 to 8-week-old BALB/c male mice, obtained from the breeding colony of the Corporación para Investigaciones Biológicas (CIB), Medellín, Colombia, were used in assays and were kept with food and water *ad libitum* (Restrepo et al., 1992). All animals were handled according to the national (Law 84 of 1989, Res No. 8430 of 1993) and international (Council of European Communities and Canadian Council of Animal Care, 1998) guidelines for animal research. The CIB research ethics committee approved the experimental protocols.

P. brasiliensis yeast cells were collected from exponentially growing batch cultures in BHI medium and counted using a hemacytometer. Animals (n=5 per isolate) were infected with *P. brasiliensis* yeast by intranasal delivery of 1.5×10^6 cells from PbWT, PbEV or *PbCATP*-aRNA strains suspended in PBS buffer. Mice were monitored daily for survival, weight loss and symptoms of disease. At 12 days post-infection, mice were euthanized and lung, liver and spleen tissues were homogenized in 2 mL PBS. Homogeneous suspensions were diluted (1:10, 1:100 and 1:1000) and 0.1 ml of each dilution was plated on Kurita's medium (Kurita et al., 1993) in order to determine the fungal burden in each organ. Plates were incubated at 36°C, 5% CO_2. CFU counts were assessed ten days after culture. The data was transformed into Log10 CFU/g of tissue.

2.9. Statistical analysis

Data are either the means or representative results of at least three experiments, each performed in triplicate. Statistical analysis and comparisons were performed using paired Student's *t* tests.

3. Results

3.1. Catalases and their deduced proteins in *Paracoccidioides* spp. and other dimorphic pathogens

We identified three catalase isoforms encoded by the genome of five strains of *Paracoccidioides* spp. representing each of the phylogenetic lineages (S1, Pb18; PS2, Pb03; PS3, PbCNH; PS4, Pb300; *P. lutzii*, Pb01), which were designated as Catalase A (*CATA*), Catalase B (*CATB*) and Catalase P (*CATP*) based on homology to known catalases reported in fungal reference genomes (Figure 1A and Table S1). Catalases in *Paracoccidioides* and other dimorphic pathogens from the Ajellomycetaceae such as *Histoplasma* and *Blastomyces* have two protein domains, the catalase activity domain (PF00199.14) and the catalase-related immune-responsive domain (PF06628.7) (Figure 1B). In addition, we found that *CATB* has an N-terminal signal peptide sequence (from 1 to 20 aa), as well as an extracellular location pattern. In *Histoplasma*, CatB is an immunodominant 90-kDa extracellular catalase highly expressed during yeast phase, also known as the M antigen-(Zancope-Oliveira et al., 1999). *CATP*, but not *CATB* and *CATA*, encodes the C-terminal

Peroxisomal Targeting Signal 1 (PTS1) ER(M/L)VASQPQSHL, suggesting a putative localization to peroxisomes for this isoform. Figure 1 shows multiple alignment, conserved domains, and phylogenetic analyses confirming the placement and conservation of *PbCATA, PbCATB* and *PbCATP*.

Since catalases have been proposed as virulence factors in dimorphic fungal pathogens, and due to the lack of genetic/functional evidence to support this in *Paracoccidioides*, we examined the molecular evolution more closely, by analyzing single nucleotide polymorphisms (SNP) between the catalases across the *Paracoccidioides* lineages. We did not find non-sense or frame shift mutations, and found a low number of SNPs in coding regions within *P. brasiliensis*, an average of 4.75 synonymous and 2 non-synonymous substitutions. However, when compared with *P. lutzii*, we found that in *CATB* there were more non-synonymous mutations than synonymous mutations. We calculated the d_N/d_S ratio as an indicator of selective pressure, and found that *CATB* has the highest d_N/d_S across the catalases (0.89) as compared with *CATA* and *CATP* (0.23 and 0.04, respectively).

In addition, we analyzed *CAT* gene family across the order Onygenales, which also includes dimorphic pathogens such as species of *Coccidioides* (family Onygenaceae) and dermatophytes (family Arthrodermataceae). We found that *CATA* and *CATP* are conserved among the Onygenales; however, *CATB* was present in the Ajellomycetaceae but not in the Onygenaceae or in the Arthrodermataceae (Figure 1A and Table S1).

3.2. Gene expression of *CAT* isoforms and *Paracoccidioides* susceptibility to H_2O_2

We measured the gene expression of the identified *CAT* isoforms in one representative isolate of each phylogenetic lineage of *Paracoccidioides* during exponential growth of the parasitic yeast and the saprophytic mycelia phases (Figure 1C). Overall, in yeast cells *CATP* was highly expressed in PbBAC and Pb60855 (both belonging to PS3), Pb03 (PS2) and Pb18 (S1), but lower levels of gene expression were detected in Pb300 (PS4) and Pb01 (*P. lutzii)*. In the mycelia, gene expression of *CATP* was generally lower compared to yeast cells for all strains, while *CATA* and *CATB* were expressed at slightly higher levels in the PS3 strains tested. The higher expression level of *CATP* in Pb18, Pb03, PbBAC and Pb60855 was correlated with the degree of susceptibility of each strain to H_2O_2. Using a disk diffusion assay we found that these strains were the less sensitive to H_2O_2 treatment *in vitro* as shown by a smaller area of clearing, which contrasts with Pb01 and Pb300 that were the most sensitive to H_2O_2 together with the lowest *CATP* expression (Figure 1D).

3.3. Kinetic expression of *CAT* isoforms in *P. brasiliensis* Pb60855 during the morphological switch

The expression profile of *CAT* isoforms was evaluated in *P. brasiliensis* cells undergoing transition [conidia to yeast (C-Y) and mycelia to yeast (M-Y)] and germination [conidia to mycelia (C-M) and yeast to mycelia (Y-M)] processes. All isoforms were present throughout the evaluated shifts, but they were differentially expressed. *PbCATP* presented lower expression levels during transition and germination processes (Figure 2), in contrast to the high expression observed during the exponential phase of growth of yeast cells (Figure 1C, Pb60855); however, *PbCATP* expression was slightly higher during the M-Y and Y-M

morphological shifts. On the other hand, *PbCATA* and *PbCATB* showed low expression levels specifically during the M-Y and Y-M morphological shifts; however, the expression level of these genes was increased during the C-Y and C-M morphological shift. *PbCATA* gene expression was higher during C-M germination, being the main isoform during this process (Figure 2).

3.4. PbCAT isoforms are differentially expressed when yeast cells are exposed to distinct oxidative stress-inducing compounds

To determine the effect of oxidative stress-inducing compounds on the expression of CAT isoforms, *P. brasiliensis* (ATCC 60855) yeast cells were treated with riboflavin, menadione (both superoxide-generating agents) (Goldberg and Stern, 1976) and H_2O_2; and co-cultured in the presence of human polymorphonuclear neutrophils (PMNs). Menadione induced a significantly increased expression of *PbCATA* and *PbCATB* as compared to the control, while riboflavin slightly induced *PbCATP*. Interaction with human PMNs induced higher expression of *PbCATA* and *PbCATP* (Figure 3). However, it is important to state that gene expression levels for all tested conditions were generally low for both *PbCATA* and *PbCATB*, as compared to the higher *PbCATP* levels, (as shown for yeast cells in Figure 1C). Upon exposure to H_2O_2, *PbCATP* was the only isoform triggered by this stimulus (up to 10-fold), as well as during interaction with human PMNs (up to 5-fold) as compared to the control (Figure 3).

3.5. Construction and analysis of a *PbCATP*-aRNA strain

Based on the signature of differential expression in response to H_2O_2 and PMN exposure, we constructed a *PbCATP*-aRNA strain in order to assess the individual contribution of this catalase to the antioxidant defenses in *P. brasiliensis*. We selected a mitotically stable strain carrying *PbCATPAS1* (Figure 4A) with the largest decrease in *PbCATP* gene expression (±50–70%) (Figure 4B). The insertion of the transfer DNA (T-DNA) into the genome of *P. brasiliensis* was confirmed via amplification of the *HPH* cassette (Figure S1). We analyzed more than one *PbCATP*-aRNA transformant and the same phenotypic features were observed. Therefore, results presented throughout the work refer to one selected aRNA strain denoted as *PbCATP*-aRNA.

Prior to performing additional assays, we analyzed the morphology, growth and vitality during batch culture of *PbCATP*-aRNA yeast cells. We did not observe morphological alterations neither at microscopic or macroscopic level as compared with PbWT or PbEV (cells transformed with the empty parental vector pUR5750) (Figure 4C). Nonetheless, we observed a decrease in biomass production of the *PbCATP*-aRNA strain after 48h (mid-exponential phase) as measured by OD and a halt in growth after 72h (Figure 4D). Also, the capacity to metabolize glucose was reduced when compared with PbWT and PbEV yeast cells (Figure 4E).

Furthermore, we analyzed the gene expression profile of other peroxide defense genes in the PbWT and *PbCATP*-aRNA strains. We evaluated the three CAT isoforms, glutathione (*GSH*) and the alternative oxidase (*AOX*) during batch culture growth. No differences were observed for any of the analyzed peroxide defense enzymes during the exponential phase of

growth of yeast cells, except as expected for *CATP* (Figure 4F), suggesting that compensatory transcriptional activation of the evaluated genes did not occur in the *PbCATP*-aRNA strain.

3.6. *PbCATP*-aRNA yeast cells are more susceptible to hydrogen peroxide

To determine if *CATP* plays an important role in the protection of *P. brasiliensis* yeast cells against H_2O_2 *in vitro*, we tested the *PbCATP*-aRNA strain for its susceptibility to this compound. *Paracoccidioides* yeast cells expressing *CATP* (PbWT and PbEV) showed similar high resistance to H_2O_2 *in vitro*, while, decreased expression of *CATP* resulted in a significantly higher susceptibility (ranging from 13.3 to 55%, with the highest difference at 1M of H_2O_2) (Figure 5A). We also evaluated the ability of extracellular and cell wall (both measuring extracellular activity) and cytoplasmic (intracellular activity) fractions of PbWT, PbEV and *PbCATP*-aRNA strains to degrade H_2O_2 *in vitro*. The *PbCATP*-aRNA strain had a decreased ability to destroy H_2O_2 but only in the intracellular fraction (Figure 5B), suggesting a role as an intracellular catalase.

3.7. *PbCATP*'s involvement during interaction with human neutrophils and in a mouse model of infection

As neutrophils are the predominant white blood cells involved in phagocytic killing of several microorganisms (Hoffbrand et al., 2007), we used these cells to test the involvement of *CATP* in phagocyte-defense. Human PMNs from healthy donors were incubated with both knockdown and wild-type yeast cells. We also inhibited NADPH oxidase from human PMNs with DPI prior to challenging with yeast cells, in order to inhibit their oxidative burst. No differences were detected in survival of *PbCATP*-aRNA yeast cells exposed to PMNs when compared to the PbWT and PbEV strains (Figure 6A). Further, we determined the gene expression levels of CAT isoforms. *PbCATA* and *PbCATB* remained unaltered after the stimulus; while, as expected, *PbCATP* in the knockdown strain had lower expression levels compared to PbWT, either in the control or upon interaction with PMNs. Additionally, we measured *AOX* and *GSH* (peroxide-defense genes), observing a slightly increased induction of *PbAOX* (Figure S2), suggesting that transcriptional compensation of this gene might occur. In contrast to the high survival of the *PbCATP*-aRNA strain in *ex vivo* assay, in a mouse model of infection a significant decrease in fungal burden of this strain was detected in mice lungs compared to the PbWT and PbEV strains (Figure 6B). Also, we recovered CFUs from the liver of mice infected with PbWT and PbEV strains, but not from tissues of mice infected with the *PbCATP*-aRNA strain (not presented in the figure due to undetected counts in knockdown). CFUs were not recovered from the spleen in any of the infected mice, irrespective of the strain used (data not shown).

Furthermore, we determined the gene expression of all CAT isoforms in the PbWT strain after interaction with human PMNs (*ex vivo*) and in yeast cells recovered from lung tissues (*in vivo*). Strikingly, we found 6.6-fold increased expression in *PbCATP* between the *ex vivo* and *in vivo* models, being significantly higher in yeast cells recovered from mice lungs. In contrast, *PbCATA* did not change, and *PbCATB* had a very slight increase (1.27-fold) (Figure 6C).

4. Discussion

Dimorphic fungal pathogens are equipped with a strong antioxidant defense system that provides them with different features and mechanisms required to efficiently establish infection and cause disease (de Oliveira et al., 2015; Perez-Nadales et al., 2014). Among these are the production of proteins that prevent host effector cells from eliciting an oxidative burst, the presence of nonenzymatic antioxidants (melanin) and the utilization of enzymatic antioxidants such as SODs and CATs, which they differentially encode and express. In the present study, we identified and characterized the three members of the CAT gene family in *Paracoccidioides* and other Onygenales. Unlike *Paracoccidioides, Histoplasma* and *Blastomyces* species, *Coccidioides* and dermatophyte genomes do not encode the extracellular catalase-*CATB* (Figure 1A). This suggests that oxidative response in the Onygenales may have evolved different mechanisms to counteract oxidative stress via catalases. In *Coccidioides*, the arthroconidia are susceptible to peroxide treatment *in vitro* (Galgiani, 1986), suggesting that the absence of *CATB* could make these cells more susceptible to host-derived ROS. In addition, *Coccidioides* spherules do not stimulate the oxidative burst of some phagocytic cells (Galgiani, 1986), implying that they would not require a large amount of catalase activity to reduce ROS (specifically peroxide) produced during the host-pathogen interactions. In spite of the absence of *CATB* in this pathogen, it has been shown that *CATP* is an up-regulated gene during the spherule parasitic phase (Whiston et al., 2012).

We studied the expression of CAT genes in different fungal strains of *Paracoccidioides* spp., covering each phylogenetic lineage (Figure 1B). Our data showed that the highest level of gene expression was detected for *CATP* in yeast cells and particularly in Pb60855, PbBAC (PS3), Pb18 (S1) and Pb03 (PS2), while the lowest levels were detected in *P. lutzii* and *P. brasiliensis* Pb300 (PS4) (both in mycelia and yeast phases). In agreement with the obtained expression data, the latter strains were the most susceptible to H_2O_2 (Figure 1D). In line with the latter results, a previous work performed at our laboratory showed that SODs expression was higher in *P. brasiliensis* strains than in *P. lutzii* (Tamayo et al., 2016); correlated with this, Pigosso and colleagues demonstrated that *P. lutzii* is metabolically more anaerobic than *P. brasiliensis* (Pigosso et al., 2013), which could be related with results obtained during the course of this work. The fact that these antioxidant gene families are expressed at different levels in the genus raises the possibility that this might have consequences for survival within the host and when facing phagocytic cells and their defensive arsenal. In line with these findings, a transcriptomic analysis performed by Edwards *et al.* using two different *Histoplasma* strains from different phylogenetic lineages, demonstrated that both of them rely on different mechanisms to survive inside the host: either the evasion of phagocyte detection or enhanced defense mechanisms (such as higher transcription of oxidative stress defense genes). They also suggested that cells in which expression of antioxidant enzymes is higher would cope and subsequently survive better to the phagocyte oxidative burst (Edwards et al., 2013). Data obtained during the course of this work together with previous studies performed in our laboratory (Tamayo et al., 2016) seems to suggest that these genetic differences in the *Paracoccidioides* genus could be behind a distinct capability to survive within the host and establish a successful pathogenic process.

Future studies should be conducted to further elucidate the role of these genetic variances in the virulence of the *Paracoccidioides* genus.

CAT genes are differentially regulated during the morphological switch and under oxidative stress-inducing conditions. *PbCATA* and *PbCATB* gene expression was higher in conidia and mycelia than in yeast cells, which might be implying that these isoforms could be important during aerobic metabolism present in mycelial cells. Moreover, according to the higher levels of *PbCATA* transcript in mycelia and during the C-M and C-Y switch, the homologous *Aspergillus nidulans* and *Neurospora crassa CATA* have been shown to be up-regulated in spores, protecting them against H_2O_2 stress and heat shock (Diaz et al., 2001; Navarro et al., 1996). Thus, these data suggest that *PbCATA* may be important during activation of conidia either in nature or once conidia infect the host and are induced to transform into the yeast pathogenic form. On the other hand, *PbCATP* transcript was higher in yeast phase (Figure 1C, bar corresponding to Pb60855) and during M-Y transition, as reported by Moreira, 2004 and Chagas, 2008 (Chagas et al., 2008; Moreira et al., 2004), overall suggesting a possible role of this during the host-pathogen interactions.

When exposed to menadione, *PbCATA* and *PbCATB* gene expression was significantly increased (Figure 3). Like-minded, menadione, besides generating superoxide anions, also increases the intracellular levels of H_2O_2 (Goldberg and Stern, 1976), implying, as it had been previously reported, that *CATA* gene expression is more correlated with endogenous oxidative stress (Chagas et al., 2008; Grossklaus et al., 2013). Further, human PMNs induced both *PbCATA* and *PbCATP* gene expression, but not *PbCATB*. Interestingly, H_2O_2 only triggered *PbCATP* gene expression (Figure 3), contrary to what we initially expected (increased gene expression of all isoforms in yeast cells treated with the catalase direct substrate), but similar to previously reported data (Chagas et al., 2008; Grossklaus et al., 2013; Moreira et al., 2004). These behaviors could be linked to the fact that these isoforms might be triggered by a specific ROS response depending on the source of stress, either endogenous (*PbCATA* and *PbCATB*) or exogenous (*PbCATP*) (Chagas et al., 2008). Considering that i) *PbCATP* gene is expressed at higher levels in exponentially growing yeast cells (Figure 1C), ii) the higher expression during M-Y transition (Figure 2), and that iii) it was the only isoform induced after stimulation of yeast cells with H_2O_2 (Figure 3), we sought to individually test the contribution of this catalase during events mimicking host-pathogen interactions. To pursue this goal, we developed a knockdown strain for *PbCATP*, using antisense RNA technology (Almeida et al., 2007; Almeida et al., 2009; Hernandez et al., 2010). We showed that a decrease in *PbCATP* gene expression significantly increased the susceptibility of *P. brasiliensis* yeast cells to H_2O_2 *in vitro* (Figures 5A and 5B), further supporting that this CAT isoform is important to detoxify this toxic molecule. Moreover, we also observed a decreased ability to destroy H_2O_2 in the intracellular fraction of the *PbCATP*-aRNA strain, but not in the extracellular or cell wall fractions. This is in agreement with data reported by Moreira *et al.* 2004 and our bioinformatic data suggesting a putative cytosolic localization of *PbCATP*, which also supports a role as an intracellular catalase. Furthermore, during batch culture growth, we observed decreased biomass production evident after 48–72 h of growth, and reduced vitality in *PbCATP*-aRNA yeast cells. It is important to consider that yeast cells are characterized by an aerobic metabolism, contributing to ROS generation. Additionally, for vitality tests we used a high concentration

of glucose. This accelerates glycolysis, stimulating ATP synthesis and leading to an additional source of ROS (S.B. Riis, 1995). The *PbCATP*-aRNA strain may be impaired and not efficiently counteract these conditions, resulting in both vitality and growth defects.

Interestingly, the decreased expression of *PbCATP* has no deleterious consequences *ex vivo*; only minor effects on yeast survival against human PMNs was observed (Figure 6A). One possibility for this result could be the fact that transcript level of *PbCATP* in the knockdown strain could be enough to maintain its survival when interacting with PMNs. Another possibility raised here is that *Paracoccidioides* cells synthesize alternative compounds, or express other enzymes in alternative pathways implicated in H_2O_2 neutralization, which might contribute to its detoxification and, in this way, promote its survival when interacting with phagocytic cells (*e.g.* melanin and expression of genes such as *AOX*, glutathione and *CCP*) (Campos et al., 2005; Hernandez et al., 2015; Parente-Rocha et al., 2015; Ruiz et al., 2011). In fact, we observed that *PbAOX* had a slightly higher induction in *PbCATP*-aRNA strain after interaction with PMNs as compared to PbWT (Figure S2), indicating that this gene might be exerting some compensatory effect to protect yeast cells, as a consequence of the decreased *PbCATP* expression. It is very likely that *CCP* could be also contributing to this compensatory effect (Parente-Rocha et al., 2015); however, we were not be able to determine the expression levels of this gene. Additionally, it is important to highlight that PMNs produce not only H_2O_2, but also other reactive species (Dahlgren and Karlsson, 1999) not directly counteracted by catalases, and this knockdown strain seemingly has only a defect to counteract H_2O_2 stress.

Similarly, although *ex vivo* experiments showed no-attenuation of the *PbCATP*-aRNA strain, the reduced gene expression of this isoform had deleterious consequences for *Paracoccidioides* virulence *in vivo*. This discrepancy between the *ex vivo* and *in vivo* models could be explained by several reasons: i) the mouse represents a much more complex environment for the fungus, and PMNs are not the only active defense mechanisms they will face; ii) *in vivo*, the oxidative burst is just one of the microbicidal strategies used by the host's defenses. Physical barriers of the lung together with the presence of other cells of the innate immunity are crucial for defense against fungal infections (Perez-Nadales et al., 2014); iii) the knockdown strain is not able to induce enough *PbCATP* levels to counteract host's defenses; iv) the oxidative burst in the granuloma might be more intense; and v) the time of interaction in the *ex vivo* experiment was just 3 h, meanwhile, in the *in vivo* model such interaction lasted days, which might have a direct effect on the survival of the fungus.

Interestingly, we found no differences in the expression levels of *PbCATA* and *PbCATB* between the *ex vivo* and *in vivo* models, but *PbCATP* gene expression was significantly higher in yeast cells recovered from mice lungs compared to those recovered upon exposure with human PMNs (6.6-fold) (Figure 6C). This fact reinforces the important role of *PbCATP* in protecting yeast cells against the deleterious effect of H_2O_2.

The presence, expression and redundancy of different antioxidant genes in *Paracoccidioides* and in other pathogenic fungi, raises the possibility that differential gene expression in the different isoforms helps to optimize the organisms' responses to environmental stresses either in nature or once within the animal host (Campos et al., 2005; Giles et al., 2006;

Johnson et al., 2002). Our results revealed that *PbCATP* is the main source of intracellular catalase activity when considering the removal of H_2O_2 generated under various environmental stresses, but also when the yeast phase expresses its pathogenic potentials. Furthermore, the response against ROS is triggered according to the source of these species, either endogenous or exogenous. Thus, *PbCATA* and *PbCATB* are triggered by endogenous signals, with both contributing to ROS homeostasis in *Paracoccidioides* cells, mainly during the conidia to yeast/mycelia switch and during defense against menadione-induced oxidative stress, while *PbCATP* is mainly triggered in the presence of exogenous ROS. Although the role of catalases in fungal virulence is not fully understood yet, this work provides new insights concerning this issue. The most significant finding was the relevance of *PbCATP* during fungal virulence *in vivo*. Thus, even if *CATP* is not essential for yeast cells under normal conditions nor during the co-incubation with human PMNs, it plays an important role in the acquisition of tolerance to some conditions set by the host.

Supplementary Material

Refer to Web version on PubMed Central for supplementary material.

Acknowledgments

This project was supported by COLCIENCIAS Colombia, grant “Silencing of genes involved in adherence and oxidative stress in *Paracoccidioides brasiliensis*: Consequences in the infectious process” (project code. 2213-52128253), and by a sustainability grant from the Universidad de Antioquia “Sostenibilidad 2015/16”. The COLCIENCIAS National Doctorate Program Funding supported DT and JFM. JFM has been supported with Federal funds from the National Institute of Allergy and Infectious Diseases, National Institutes of Health, Department of Health and Human Services, under Grant Number U19AI110818 to the Broad Institute.

References

Almeida AJ, et al. Towards a molecular genetic system for the pathogenic fungus Paracoccidioides brasiliensis. Fungal Genet Biol. 2007; 44:1387–98. [PubMed: 17512227]

Almeida AJ, et al. Cdc42p controls yeast-cell shape and virulence of Paracoccidioides brasiliensis. Fungal Genet Biol. 2009; 46:919–26. [PubMed: 19686860]

Altschul SF, et al. Gapped BLAST and PSI-BLAST: a new generation of protein database search programs. Nucleic Acids Res. 1997; 25:3389–402. [PubMed: 9254694]

Beijersbergen A, et al. Conjugative Transfer by the Virulence System of Agrobacterium tumefaciens. Science. 1992; 256:1324–7. [PubMed: 17736763]

Boyce KJ, Andrianopoulos A. Fungal dimorphism: the switch from hyphae to yeast is a specialized morphogenetic adaptation allowing colonization of a host. FEMS Microbiol Rev. 2015; 39:797–811. [PubMed: 26253139]

Buitrago MJ, Cuenca-Estrella M. Current epidemiology and laboratory diagnosis of endemic mycoses in Spain. Enferm Infecc Microbiol Clin. 2012; 30:407–13. [PubMed: 22130575]

Campos EG, et al. Oxidative stress response in Paracoccidioides brasiliensis. Genet Mol Res. 2005; 4:409–29. [PubMed: 16110454]

Chagas RF, et al. Purification of Paracoccidioides brasiliensis catalase P: subsequent kinetic and stability studies. J Biochem. 2010; 147:345–51. [PubMed: 19897569]

Chagas RF, et al. The catalases of Paracoccidioides brasiliensis are differentially regulated: protein activity and transcript analysis. Fungal Genet Biol. 2008; 45:1470–8. [PubMed: 18799136]

Chelikani P, et al. Diversity of structures and properties among catalases. Cell Mol Life Sci. 2004; 61:192–208. [PubMed: 14745498]

Colombo AL, et al. Epidemiology of endemic systemic fungal infections in Latin America. Med Mycol. 2011; 49:785–98. [PubMed: 21539506]

Dahlgren C, Karlsson A. Respiratory burst in human neutrophils. J Immunol Methods. 1999; 232:3–14. [PubMed: 10618505]

de Oliveira HC, et al. Paracoccidioides-host Interaction: An Overview on Recent Advances in the Paracoccidioidomycosis. Front Microbiol. 2015; 6:1319. [PubMed: 26635779]

den Dulk-Ras A, Hooykaas PJ. Electroporation of Agrobacterium tumefaciens. Methods Mol Biol. 1995; 55:63–72. [PubMed: 8528423]

Desjardins CA, et al. Comparative genomic analysis of human fungal pathogens causing paracoccidioidomycosis. PLoS Genet. 2011; 7:e1002345. [PubMed: 22046142]

Diaz A, et al. Molecular and kinetic study of catalase-1, a durable large catalase of Neurospora crassa. Free Radic Biol Med. 2001; 31:1323–33. [PubMed: 11728803]

Edgar RC. MUSCLE: multiple sequence alignment with high accuracy and high throughput. Nucleic Acids Res. 2004; 32:1792–7. [PubMed: 15034147]

Edwards JA, et al. Histoplasma yeast and mycelial transcriptomes reveal pathogenic-phase and lineage-specific gene expression profiles. BMC Genomics. 2013; 14:695. [PubMed: 24112604]

Emanuelsson O, et al. Predicting subcellular localization of proteins based on their N-terminal amino acid sequence. J Mol Biol. 2000; 300:1005–16. [PubMed: 10891285]

Galgiani JN. Inhibition of different phases of Coccidioides immitis by human neutrophils or hydrogen peroxide. J Infect Dis. 1986; 153:217–22. [PubMed: 3944479]

Garcia AM, et al. Identification of genes associated with germination of conidia to form mycelia in the fungus Paracoccidioides brasiliensis. Biomedica. 2009; 29:403–12. [PubMed: 20436992]

Gegembauer G, et al. Serology of paracoccidioidomycosis due to Paracoccidioides lutzii. PLoS Negl Trop Dis. 2014; 8:e2986. [PubMed: 25032829]

Giles SS, et al. The Cryptococcus neoformans catalase gene family and its role in antioxidant defense. Eukaryot Cell. 2006; 5:1447–59. [PubMed: 16963629]

Goldberg B, Stern A. Production of superoxide anion during the oxidation of hemoglobin by menadione. Biochim Biophys Acta. 1976; 437:628–32. [PubMed: 182230]

Goldman GH, et al. Expressed sequence tag analysis of the human pathogen Paracoccidioides brasiliensis yeast phase: identification of putative homologues of Candida albicans virulence and pathogenicity genes. Eukaryot Cell. 2003; 2:34–48. [PubMed: 12582121]

Grossklaus DD, et al. Response to oxidative stress in Paracoccidioides yeast cells as determined by proteomic analysis. Microbes and Infection. 2013; 15:347–364. [PubMed: 23421979]

Hahn RC, et al. Fatal fungemia due to Paracoccidioides lutzii. Am J Trop Med Hyg. 2014; 91:394–8. [PubMed: 24821845]

Henriet SS, et al. Human leukocytes kill Aspergillus nidulans by reactive oxygen species-independent mechanisms. Infect Immun. 2011; 79:767–73. [PubMed: 21078850]

Hernandez O, et al. A 32-kilodalton hydrolase plays an important role in Paracoccidioides brasiliensis adherence to host cells and influences pathogenicity. Infect Immun. 2010; 78:5280–6. [PubMed: 20876288]

Hernandez O, et al. Alternative oxidase plays an important role in Paracoccidioides brasiliensis cellular homeostasis and morphological transition. Med Mycol. 2015; 53:205–14. [PubMed: 25631476]

Hernandez O, et al. Gene expression during activation of Paracoccidioides brasiliensis conidia. Yeast. 2011a; 28:771–81. [PubMed: 21960298]

Hernandez O, et al. Kinetic analysis of gene expression during mycelium to yeast transition and yeast to mycelium germination in Paracoccidioides brasiliensis. Biomedica. 2011b; 31:570–9. [PubMed: 22674368]

Hoffbrand V, et al. Postgraduate Haematology. 2007

Holbrook ED, et al. Redundant catalases detoxify phagocyte reactive oxygen and facilitate Histoplasma capsulatum pathogenesis. Infect Immun. 2013; 81:2334–46. [PubMed: 23589579]

Imlay JA, et al. Toxic DNA damage by hydrogen peroxide through the Fenton reaction in vivo and in vitro. Science. 1988; 240:640–2. [PubMed: 2834821]

Johnson CH, et al. Redundancy, phylogeny and differential expression of Histoplasma capsulatum catalases. Microbiology. 2002; 148:1129–42. [PubMed: 11932457]

Kara BV, Daoud I, Searle B. European Bravery Convention. Proceedings of the 21st Congress. 1987

Kurita N, et al. An improved culture medium for detecting live yeast phase cells of Paracoccidioides brasiliensis. J Med Vet Mycol. 1993; 31:201–5. [PubMed: 8360811]

Lambou K, et al. Functional analysis of the superoxide dismutase family in Aspergillus fumigatus. Mol Microbiol. 2010; 75:910–23. [PubMed: 20487287]

Lander ES, et al. Initial sequencing and analysis of the human genome. Nature. 2001; 409:860–921. [PubMed: 11237011]

Li L, et al. OrthoMCL: identification of ortholog groups for eukaryotic genomes. Genome Res. 2003; 13:2178–89. [PubMed: 12952885]

Loew O. A New Enzyme of General Occurrence in Organismis. Science. 1900; 11:701–2. [PubMed: 17751716]

Lushchak VI. Adaptive response to oxidative stress: Bacteria, fungi, plants and animals. Comp Biochem Physiol C Toxicol Pharmacol. 2011; 153:175–90. [PubMed: 20959147]

Martinez R. Epidemiology of Paracoccidioidomycosis. Rev Inst Med Trop Sao Paulo. 2015; 57(Suppl 19):11–20. [PubMed: 26465364]

Martins VP, et al. Involvement of an alternative oxidase in oxidative stress and mycelium-to-yeast differentiation in Paracoccidioides brasiliensis. Eukaryot Cell. 2011; 10:237–48. [PubMed: 21183691]

Matute DR, et al. Cryptic speciation and recombination in the fungus Paracoccidioides brasiliensis as revealed by gene genealogies. Mol Biol Evol. 2006; 23:65–73. [PubMed: 16151188]

Mejia SP, et al. Human neutrophils produce extracellular traps against Paracoccidioides brasiliensis. Microbiology. 2015

Missall TA, et al. Mechanisms of resistance to oxidative and nitrosative stress: implications for fungal survival in mammalian hosts. Eukaryot Cell. 2004; 3:835–46. [PubMed: 15302816]

Moreira SF, et al. Monofunctional catalase P of Paracoccidioides brasiliensis: identification, characterization, molecular cloning and expression analysis. Yeast. 2004; 21:173–82. [PubMed: 14755642]

Munoz JF, et al. Genome Diversity, Recombination, and Virulence across the Major Lineages of Paracoccidioides. mSphere. 2016:1.

Munoz JF, et al. Genome update of the dimorphic human pathogenic fungi causing paracoccidioidomycosis. PLoS Negl Trop Dis. 2014; 8:e3348. [PubMed: 25474325]

Munoz JF, et al. The Dynamic Genome and Transcriptome of the Human Fungal Pathogen Blastomyces and Close Relative Emmonsia. PLoS Genet. 2015; 11:e1005493. [PubMed: 26439490]

Navarro RE, et al. catA, a new Aspergillus nidulans gene encoding a developmentally regulated catalase. Curr Genet. 1996; 29:352–9. [PubMed: 8598056]

Neuberger G, et al. Prediction of peroxisomal targeting signal 1 containing proteins from amino acid sequence. J Mol Biol. 2003; 328:581–92. [PubMed: 12706718]

Parente-Rocha JA, et al. Macrophage Interaction with Paracoccidioides brasiliensis Yeast Cells Modulates Fungal Metabolism and Generates a Response to Oxidative Stress. PLoS One. 2015; 10:e0137619. [PubMed: 26360774]

Perez-Nadales E, et al. Fungal model systems and the elucidation of pathogenicity determinants. Fungal Genet Biol. 2014; 70:42–67. [PubMed: 25011008]

Petersen TN, et al. SignalP 4.0: discriminating signal peptides from transmembrane regions. Nat Methods. 2011; 8:785–6. [PubMed: 21959131]

Pigosso LL, et al. Comparative proteomics in the genus Paracoccidioides. Fungal Genet Biol. 2013; 60:87–100. [PubMed: 23911955]

Rappleye CA, et al. RNA interference in Histoplasma capsulatum demonstrates a role for alpha-(1,3)-glucan in virulence. Mol Microbiol. 2004; 53:153–65. [PubMed: 15225311]

Restrepo A, et al. A technique to collect and dislodge conidia produced by Paracoccidioides brasiliensis mycelial form. J Med Vet Mycol. 1986; 24:247–50. [PubMed: 3735034]

Restrepo S, et al. Development of pulmonary fibrosis in mice during infection with Paracoccidioides brasiliensis conidia. J Med Vet Mycol. 1992; 30:173–84. [PubMed: 1517956]

Robinson JM, et al. Regulation of the NADPH-oxidase complex of phagocytic leukocytes. Recent insights from structural biology, molecular genetics, and microscopy. Histochem Cell Biol. 2004; 122:293–304. [PubMed: 15365846]

Ruane PH, et al. Photochemical inactivation of selected viruses and bacteria in platelet concentrates using riboflavin and light. Transfusion. 2004; 44:877–85. [PubMed: 15157255]

Ruiz OH, et al. Alternative oxidase mediates pathogen resistance in Paracoccidioides brasiliensis infection. PLoS Negl Trop Dis. 2011; 5:e1353. [PubMed: 22039556]

Riis SB, Pedersen HM, Sørensen NK, Jakobsen M. Flow cytometry and acidification power test as rapid techniques for determination of the activity of starter cultures of Lactobacillus delbrueckii ssp. bulgaricus. Food Microbiology. 1995; 12:245–250.

Saitou N, Nei M. The neighbor-joining method: a new method for reconstructing phylogenetic trees. Mol Biol Evol. 1987; 4:406–25. [PubMed: 3447015]

Scorzoni L, et al. Comparison of virulence between Paracoccidioides brasiliensis and Paracoccidioides lutzii using Galleria mellonella as a host model. Virulence. 2015; 6:766–76. [PubMed: 26552324]

Sifuentes-Osornio J, et al. Epidemiology of Invasive Fungal Infections in Latin America. Curr Fungal Infect Rep. 2012; 6:23–34. [PubMed: 22363832]

Tamayo D, et al. Identification and Analysis of the Role of Superoxide Dismutases Isoforms in the Pathogenesis of Paracoccidioides spp. PLoS Negl Trop Dis. 2016; 10:e0004481. [PubMed: 26963091]

Teixeira MM, et al. Phylogenetic analysis reveals a high level of speciation in the Paracoccidioides genus. Mol Phylogenet Evol. 2009; 52:273–83. [PubMed: 19376249]

Teixeira MM, et al. Paracoccidioides species complex: ecology, phylogeny, sexual reproduction, and virulence. PLoS Pathog. 2014; 10:e1004397. [PubMed: 25357210]

Vacca RA, et al. Production of reactive oxygen species, alteration of cytosolic ascorbate peroxidase, and impairment of mitochondrial metabolism are early events in heat shock-induced programmed cell death in tobacco Bright-Yellow 2 cells. Plant Physiol. 2004; 134:1100–12. [PubMed: 15020761]

Whiston E, et al. Comparative transcriptomics of the saprobic and parasitic growth phases in Coccidioides spp. PLoS One. 2012; 7:e41034. [PubMed: 22911737]

Youseff BH, et al. Extracellular superoxide dismutase protects Histoplasma yeast cells from host-derived oxidative stress. PLoS Pathog. 2012; 8:e1002713. [PubMed: 22615571]

Zancope-Oliveira RM, et al. Molecular cloning, characterization, and expression of the M antigen of Histoplasma capsulatum. Infect Immun. 1999; 67:1947–53. [PubMed: 10085041]

Zdobnov EM, Apweiler R. InterProScan–an integration platform for the signature-recognition methods in InterPro. Bioinformatics. 2001; 17:847–8. [PubMed: 11590104]

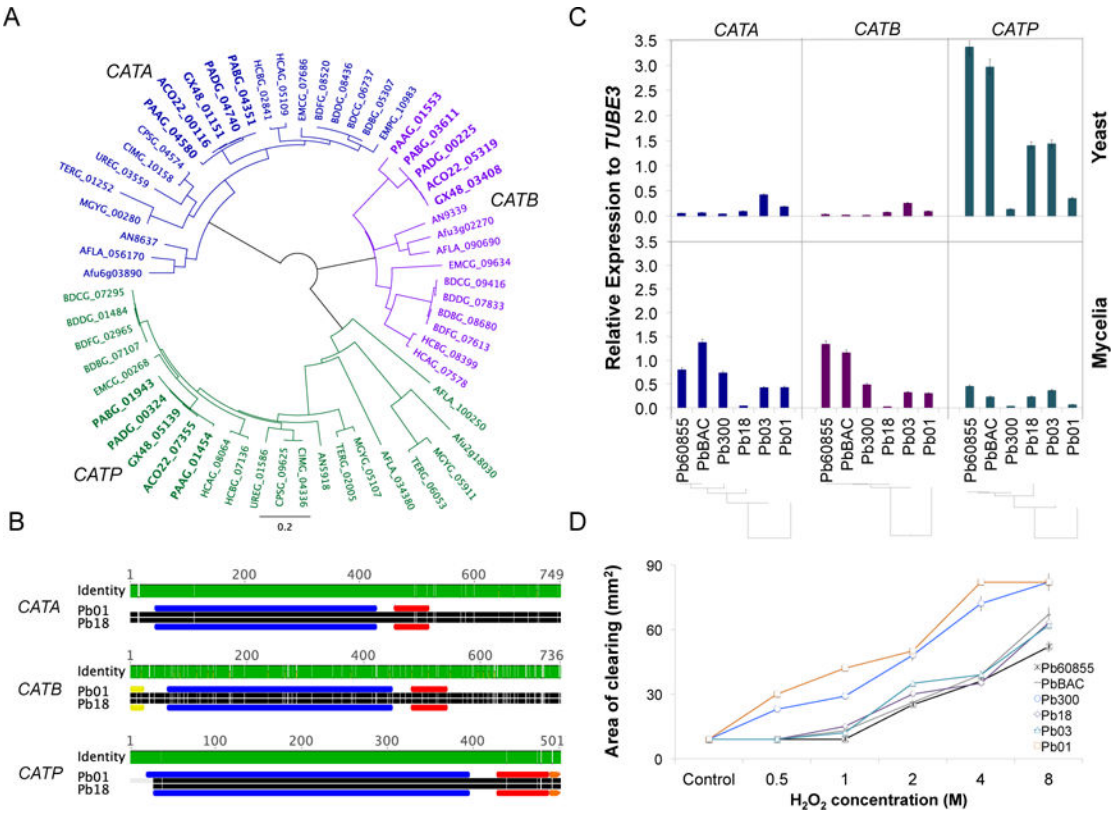

Figure 1. Identification and gene expression of *Paracoccidioides* spp catalases, and susceptibility to H_2O_2

(A) Phylogenetic tree of CAT isoforms (*CATA*, *CATB*, *CATP*) encoded by the genome of *Paracoccidioides* (gene IDs in bold) and Onygenales such as *Histoplasma*, *Blastomyces*, *Coccidioides*, and dermatophytes; outgroup *Aspergillus*. **(B)**, Functional annotation and protein domains of identified CATs in *Paracoccidioides*. The catalase activity domain (PF00199.14) is presented in blue, and the immune-responsive domain (PF06628.7) in red. The predicted secreted signal and the peroxisomal targeting signal are presented in yellow and orange, respectively. Green or white lines across the proteins represent high level of identity or low level of identity for each position of the alignment, respectively. **(C)** Expression profile of CAT isoforms in yeast phase (36°C) and mycelia phase (20°C) during exponential growth. **(D)** Susceptibility of *Paracoccidioides* yeast cells to peroxide (H_2O_2). Cells were exposed to increasing concentrations of this compound and the inhibition zone was determined as the area lacking yeast cell growth. The chosen strains represent the phylogenetic lineages of *Paracoccidioides* spp. (PS4: Pb300; PS3: Pb60855 and PbBAC; PS2: Pb03; S1: Pb18, and *P. lutzii*: Pb01).

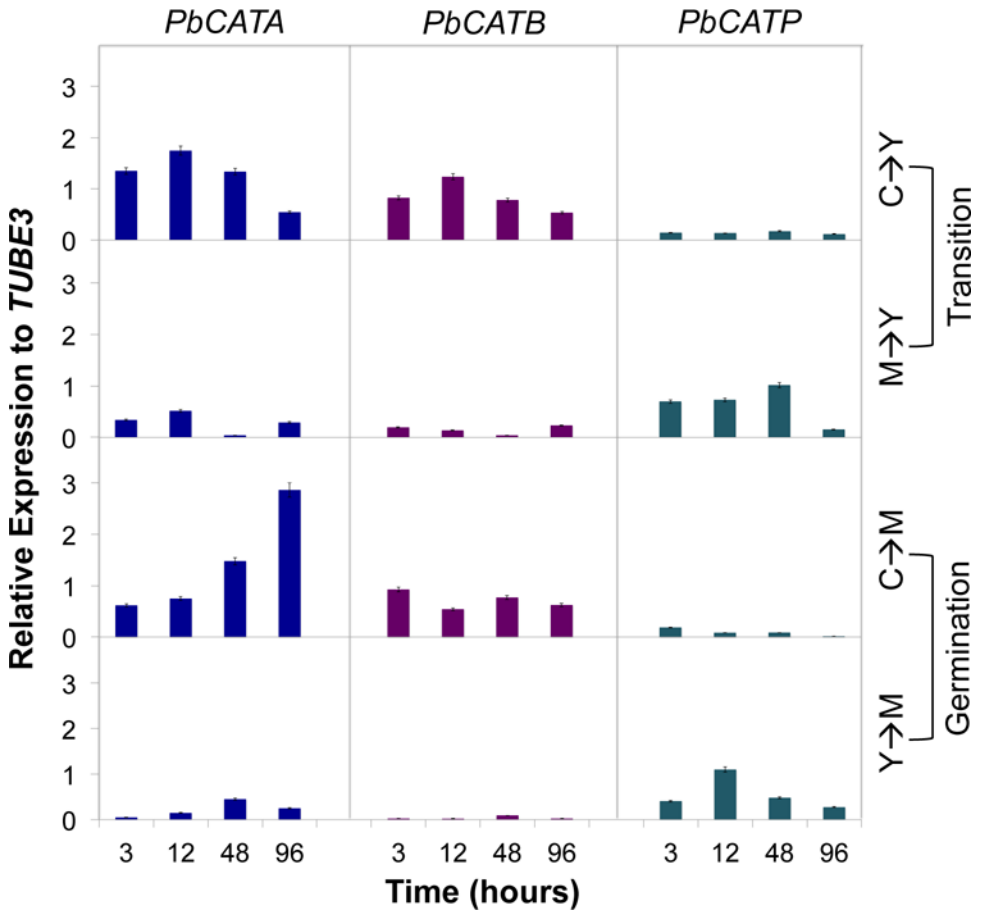

Figure 2. Gene expression of CAT isoforms in Pb60855

Expression of CAT isoforms was determined during transition (C-Y and M-Y) and also during germination (C-M and Y-M). *P. brasiliensis* cells were inoculated in BHI liquid medium kept at 36°C and 20°C in order to induce the transition and germination processes, respectively. Gene expression levels of CAT isoforms were determined at 3, 12, 48 and 96 h, and were obtained by RT-qPCR assay. The measurement was normalized with the housekeeping gene β-tubulin.

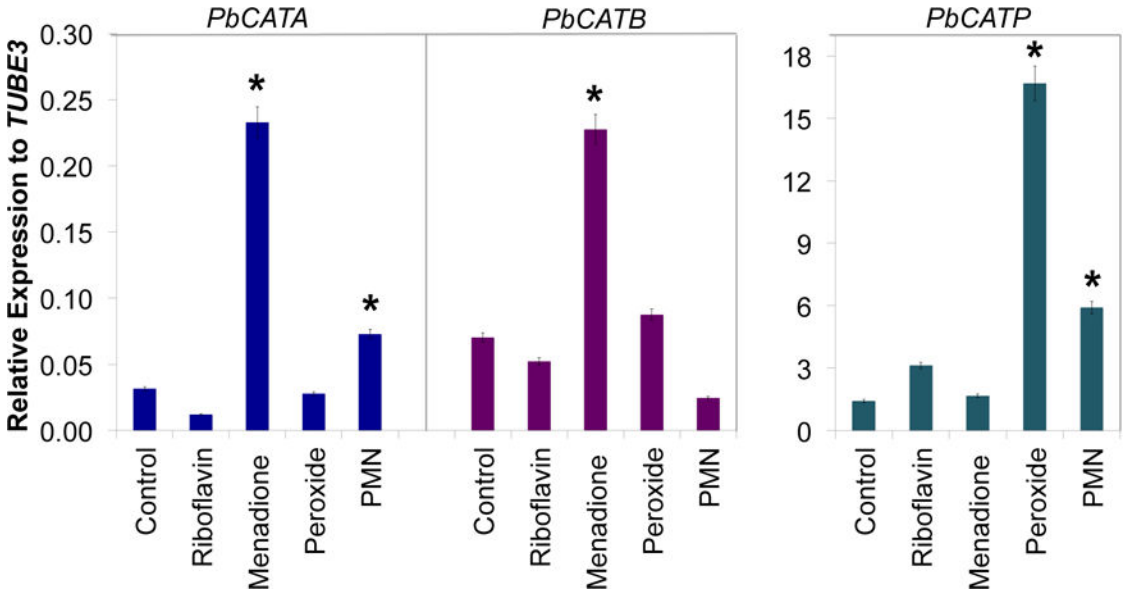

Figure 3. Expression of PbCAT isoforms during exposure to oxidative stress-inducing compounds

P. brasiliensis yeast cells were exposed to menadione, peroxide (H_2O_2) and riboflavin for 1 hour. For interaction with human PMNs, yeast cells were co-cultivated during 3 hours. Gene expression levels of CAT isoforms were obtained by RT-qPCR. The measurement was normalized with the housekeeping gene β-tubulin. Results are the mean of three individual experiments. Asterisks denote $p \leq 0.05$ compared to control cells.

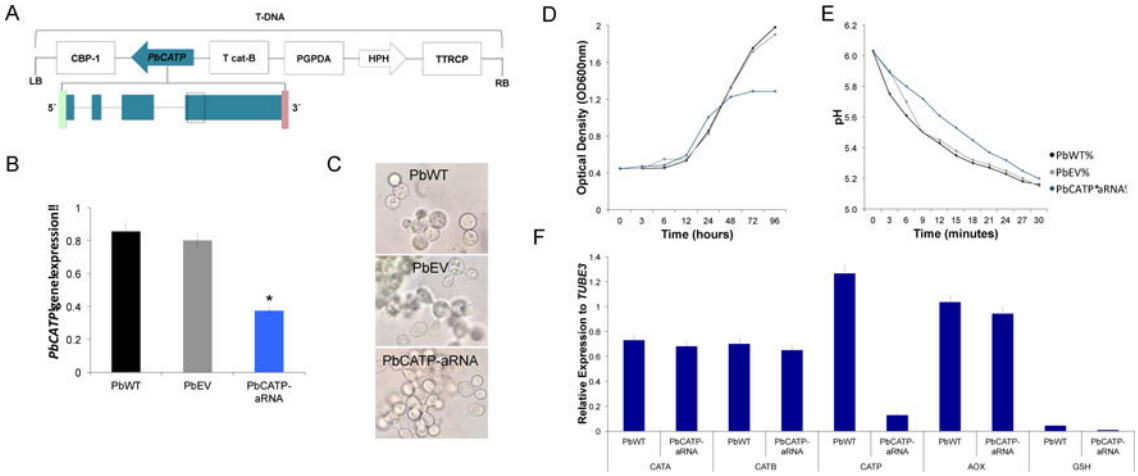

Figure 4. *CATP* gene silencing in *P. brasiliensis*

(A) Transfer DNA (T-DNA) inserted into the genome of *P. brasiliensis* yeast cells via ATMT. The antisense oligonucleotide was targeted to exon four (dashed box), with a length of 80 bp. This AS oligonucleotide was placed under control of the calcium binding protein (*CBP*-1), the terminator *CAT*-B and harboring hygromycin B phosphotransferase (*HPH*) under control of *Aspergillus nidulans* glyceraldehyde 3-phosphate (*PGPDA*) and with the terminator *TTRCP*. **(B) *PbCATP*** gene expression levels obtained by RT-qPCR assay. The measurement was normalized with the housekeeping gene β-tubulin in the wild-type (PbWT60855), the empty vector control (PbEV60855) and the antisense RNA strain (Pb*CATP*-aRNA) grown at exponential phase. Mitotic stability was confirmed by sub-culturing *P. brasiliensis PbCATP*-aRNA yeast cells, checking for low expression levels in this isolate after successive sub-cultures. **(C)** Light microscopy of *P. brasiliensis* yeast cells morphology. **(D)** Growth curve in PbWT60855, PbEV60855, *PbCATP*-aRNA. Yeast cells were grown in BHI liquid medium at 36°C, OD600 nm was determined at each time point. **(E)** Vitality in PbWT60855, PbEV60855 and *PbCATP*-aRNA. The pH change was monitored in yeast suspensions at three minutes intervals, for 30 minutes. Results represent the mean of three individual experiments. **(F)** Profile expression of CAT isoforms, alternative oxidase (*AOX*) and glutathione (*GSH*) in PbWT and *PbCATP*-aRNA yeast cells during batch culture growth. Gene expression levels were determined by RT-qPCR assay and normalized with the housekeeping gene β-tubulin. Results are the mean of three individual experiments.

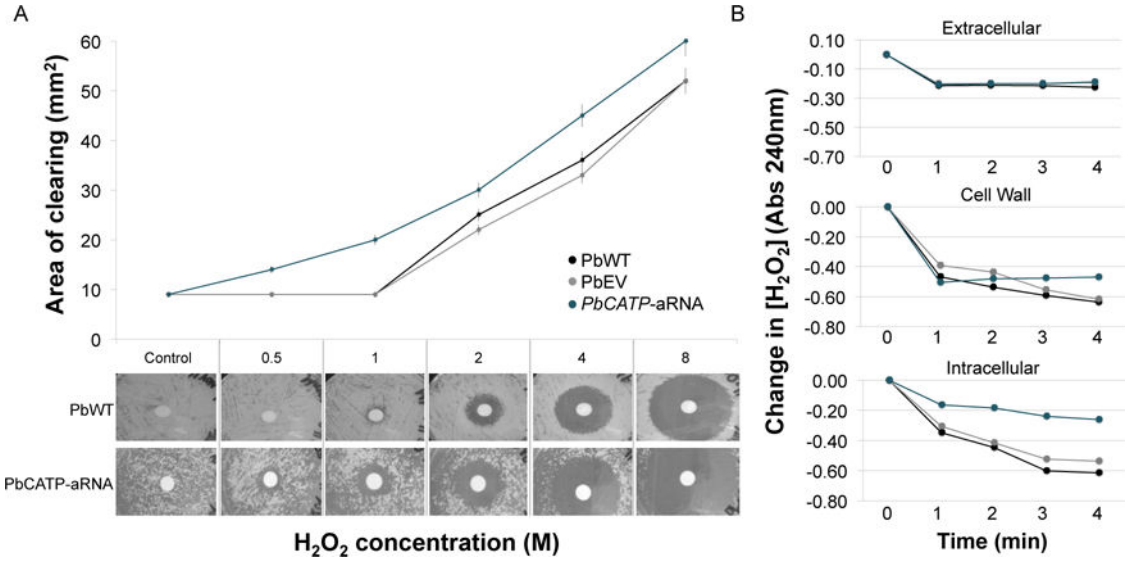

Figure 5. Exposure of *CATP* knockdown strain to hydrogen peroxide

(A) Quantification of the sensitivity to H_2O_2 in *P. brasiliensis* yeast cells. Yeast cells were exposed to increasing concentrations of this compound and the inhibition zone was determined as the area lacking yeast cell growth. (**Top**) Data presented correspond to the average for three replicate tests, with error bars representing standard deviations. (**Bottom**) Images of *P. brasiliensis* growth around H_2O_2 saturated disks. Saturated filter disks without H_2O_2 as control, and 0.5 to 8 M H_2O_2. **(B)** Determination of the ability of *P. brasiliensis* yeast cells to degrade H_2O_2. Extracellular, cell wall and cytoplasmic fractions from PbWT, PbEV and *PbCATP*-aRNA strains were collected. Relative H_2O_2 destruction was measured as the decrease in the absorbance at 240 nm. Results are the mean of three individual experiments.

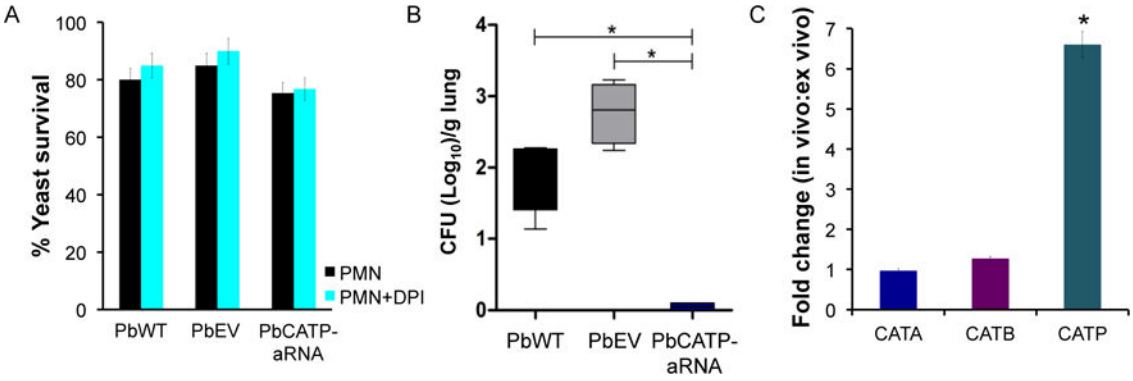

Figure 6. Effect of *CATP* decreased expression in an *ex vivo* and *in vivo* models of infection

(A) *P. brasiliensis* yeast cells were incubated in the presence of human PMNs for 3 hours, at 36 °C, with 5% of CO_2. Then, yeast cells survival was determined by enumeration of viable CFUs (black bar). Later on, human PMNs were treated with DPI (blue bar) in order to inhibit NADPH-oxidase. Next, yeast survival was determined during the interaction of *P. brasiliensis* with human PMNs treated with DPI. **(B)** Virulence of *PbCATP*-aRNA isolate in an experimental murine model of infection. CFUs recovered from lungs of mice intranasally inoculated with 1.5×10^6 yeast cells obtained from PbWT, PbEV, and *PbCATP*-aRNA strains. Mice were euthanized at 12 days post-infection, their organs were harvested and the fungal burden in lung tissue was determined. No significant differences between the PbWT and PbEV strains were found. Asterisks indicate significant differences ($p < 0.05$) from animals infected with PbWT and PbEV as compared to *PbCATP*-aRNA strains determined by Student's *t* test. (**C**) Expression of CAT isoforms in yeast cells from PbWT obtained after interaction with PMNs (*ex vivo*) and in yeast cells recovered from lung tissues (*in vivo*). Bars represent the fold changes (*in vivo* compared to *ex vivo* gene expression) for *PbCATA, PbCATB* and *PbCATP* genes, determined through RT-qPCR assay and normalized with the housekeeping gene β-tubulin.

Table 1

Strains used in this study.

Species	Strain designation	Phylogenetic lineage
P. brasiliensis	Pb18	S1
P. brasiliensis	Pb03	PS2
P. brasiliensis	Pb60855, PbBAC	PS3
P. brasiliensis	Pb300	PS4
P. lutzii	Pb01	*Pb01*-like
P. brasiliensis	PbEV *	PS3
P. brasiliensis	*PbCATP*-aRNA *	PS3
A. tumefaciens	*LBA1100*	N/A
E. coli	*DH5*-α	N/A

* Background strain Pb60855

N/A: Not apply